NASA Technical Memorandum 100093

Experimental Program for Real Gas Flow Code Validation at NASA Ames Research Center

George S. Deiwert, Anthony W. Strawa,
Surendra P. Sharma, and Chul Park

July 1989

National Aeronautics and
Space Administration

NASA Technical Memorandum 100093

Experimental Program for Real Gas Flow Code Validation at NASA Ames Research Center

George S. Deiwert, Anthony W. Strawa, Surendra P. Sharma, and Chul Park
Ames Research Center, Moffett Field, California

July 1989

NASA

National Aeronautics and
Space Administration

Ames Research Center
Moffett Field, California 94035

EXPERIMENTAL PROGRAM FOR REAL GAS FLOW CODE VALIDATION AT NASA AMES RESEARCH CENTER

by

George S. Deiwert, Anthony W. Strawa, Surendra P. Sharma, and Chul Park
Aerothermodynamics Branch
NASA Ames Research Center, Moffett Field, California 94035 USA

SUMMARY

The experimental program for validating real gas hypersonic flow codes at NASA Ames Research Center is described. Ground-based test facilities used include ballistic ranges, shock tubes and shock tunnels, arc jet facilities and heated-air hypersonic wind tunnels. Also included are large-scale computer systems for kinetic theory simulations and benchmark code solutions. Flight tests consist of the Aeroassist Flight Experiment, the Space Shuttle, Project Fire 2, and planetary probes such as Galileo, Pioneer Venus, and PAET.

INTRODUCTION

Computational fluid dynamics involves the numerical solution of the equations of motion which describe the conservation of mass, momentum, and energy. The most general forms of these equations are the compressible Navier-Stokes equations for continuum flight regimes and the Boltzmann equation for rarefied flight regimes. Many continuum flow fields have been well simulated for a variety of shapes and flow conditions where strong viscous/inviscid interactions and/or flow separation are important by advancing these equations in time until a steady state is asymptotically achieved. When there is no flow reversal and the flow in the streamwise direction is supersonic, these equations can be simplified by neglecting the streamwise viscous terms. The solution to these simplified equations, referred to as the parabolized Navier-Stokes equations, can be found by efficient streamwise marching techniques. Further simplification can be achieved, when viscous/inviscid interactions are weak, by decoupling the viscous and inviscid dominated regions from one another and simulating the regions separately in an iterative manner. Here the inviscid Navier-Stokes equations, termed the Euler equations, are solved in the inviscid region away from body surfaces. Near the body surface, the viscous dominated boundary layer equations are solved. A fourth simplification which can be used for strong viscous/inviscid interactions is the viscous shock layer approximation. This method is used for the stagnation region of hypersonic blunt bodies between the bow shock and the body surface.

Real gas effects include thermochemical nonequilibrium, where finite rate processes for chemical and energy exchange phenomena occur, and radiative transport is a coupled process. To account for chemical reactions, conservation equations for each chemical species must be added to the flow-field equation set. There are five flow-field equations (one continuity, three momentum, and one energy equation). For dissociating and ionizing air, there are typically 11 species (N_2, O_2, N, O, NO, O^+, N^+, NO^+,N_2^+, O_2^+, and e^-). The inclusion of conservation equations for each of these species nearly triples the number of equations to be solved. When there are combustion processes or gas/surface interactions or ablation products, the number of species increases dramatically. To account for thermal nonequilibrium and radiative transport, there are additional energy equations to describe the energy exchange between the various energy modes (such as translational, rotational, vibrational, and electronic). To further complicate the analysis, the range of time scales involved in thermochemical processes is many orders of magnitude wider than the mean flow time scale. This is the single most complicating factor in computational aerothermodynamics. Coupled radiative transport results in a system of integrodifferential equations which are exceedingly difficult to solve. Simplifying assumptions (such as either optical transparency, or gray gas, or tangent slab models) are generally used to reduce this level of complexity. Many varieties of simplifications are used to alleviate problems associated with widely disparate time scales and are discussed briefly next.

Many flows can be adequately approximated by assuming an equilibrium real gas. Here all the reaction rates are assumed to be fast enough so that the gas is everywhere in local equilibrium, and the thermochemical state of the gas can be defined solely by the local temperature and pressure. Reactions are allowed to occur and effect the solution only through the equation of state of the equilibrium gas mixture. This is a good approximation for higher-pressure, lower-altitude cases, and it can be used for a major portion of the analysis of such vehicles as hypersonic aircraft which fly in the sensible part of the atmosphere. In the other extreme, reactions are sometimes so slow that the gas can be considered frozen in a particular chemical state. This phenomenon frequently occurs in regions of rapid expansion such as in jets or base regions of body shapes, but the frozen gas model can sometimes be used behind compressive shocks as well.

When finite rate chemical reactions are important, they can often be considered to be in thermal equilibrium. That is, the energy modes of the species equilibrate very rapidly compared to the chemical rate processes. Even with this simplification the chemical rate time scales vary over an extremely wide range, resulting in a "stiff" behavior of the complete equation set and adding to the difficulty in solving the flow field and species equations in a fully coupled manner. In these cases the species equations are often effectively uncoupled from the flow-field equations and solved separately in a "loosely" coupled manner, often by a different (usually implicit) numerical technique. To validate these real gas codes, both ground- based and flight experiments are necessary to assess the effects of chemical kinetics, high enthalpy, low density, and scale.

In the past, ground-based test facilities (such as shock tubes, arc jets, and ballistic ranges) were used, in conjunction with engineering design and analysis codes, to achieve closure on designs of such vehicles as Apollo, the Space Shuttle, and the Galileo probe. Ground-based test facilities can provide valuable insight for the design and understanding of aerospace vehicles but cannot simulate all of the conditions (combinations of scale, altitude, and velocity) that will be encountered in planned missions of the future. Today, these facilities are being used to provide validation data for real gas flow codes which are, in turn, used to simulate actual flight conditions. Photographs of some of these facilities are shown in Fig. 1. The simulation capability of these facilities as a function of length Reynolds number, flight velocity, and enthalpy is shown in Fig. 2. The facilities represented in this figure are: (1) The Hypersonic Free-Flight Aerodynamic Facility (HFFAF), a countercurrent ballistic range which can also be operated as a Mach 7 shock tunnel with sting mounted models, and as a ballistic free-flight range with a quiescent gas;, (2) the Electric Arc Shock Tube (EAST) Facility; (3) the 60-MW Interaction Heating Facility; and (4) the 3.5-Foot Hypersonic Wind Tunnel (HWT). Also shown are the flight regimes for the Space Shuttle and for the Aeroassist Flight Experiment (AFE). Indicated in the figure are regimes where various real gas phenomena become important, such as slip-flow and free-molecular-flow regimes, the dissociation of oxygen and nitrogen, and

ionization. Superimposed are trajectories of typical hypersonic aerospace vehicles including the Space Shuttle, boost glide vehicle (BGV), a transatmospheric vehicle (TAV), and an aeroassisted orbital transfer vehicle (AOTV).

The operating characteristics of each of the test facilities, how each relates to the flight regimes of various aerospace vehicles, the type of data each can produce with appropriate instrumentation, and how each can be used for code validation, are covered in this paper. Both ground-based tests and flight tests can provide valuable data to validate computational methods. The computational methods can then, in turn, be used to extrapolate our understanding and analysis into regimes not covered by existing facilities.

A summary of the experimental activity and its relationship to the validation of real gas flow codes is shown in Table 1. Here the flow codes have been summarized by six generic classes: (1) perfect gas hypersonic upwind codes, (2) real gas upwind codes, (3) real gas nozzle/plume codes, (4) hydrogen-air combustion codes, (5) multi-temperature thermochemical nonequilibium codes, and (6) hypersonic transition and boundary layer codes. A discussion of this activity follows in the next section, and is identified by each experimental facility.

EXPERIMENTAL PROGRAM

Ballistic Range Tests

Ballistic ranges can be used to achieve flight velocities where real gas effects are important. They offer an advantage over other hypersonic facilities in that the free-stream conditions are known and there are no model supports to cause interference, particularly in the base region. This simplifies boundary and initial conditions used in computations and eliminates one source of ambiguity between computational and experimental results.

Two ballistic range facilities at Ames Research Center support hypersonic research: The Hypersonic Free-Flight Aerodynamic Facility (HFFAF), and the Pressurized Ballistic Range (PBR). These two facilities compliment each other, each having specific advantages for certain types of tests. Together, they allow testing of a variety of models over a wide range of density, speed, and Reynolds number. Each facility and associated experiments is described briefly.

Hypersonic Free-Flight Aerodynamic Facility (HFFAF). A photograph and schematic of the HFFAF are shown in Fig. 3. The free-flight test section is 23 m long and has 16 orthogonal spark shadowgraph stations evenly spaced (1.52 m) over its length. Kerr-cell shutters are used to produce a sharp model and flow-field image on the film. Four deformable-piston, light-gas guns, having bore diameters of 0.71, 1.27, 2.54, and 3.81 cm, are available for launching the model into free flight. Each of these guns can operate to muzzle velocities of about 9 km/sec. A shock tunnel to provide a countercurrent flow capability is currently being reactivated.

Tests in this facility can be conducted from as high as 1 atm to as low as about 0.02 Torr, and in nontoxic gases other than air, such as CO_2, H_2, He, Kr, and Xe. The details of the operating characteristics of this facility are described in detail in Ref. 1, and are summarized in Table 2.

Pressurized Ballistic Range. The PBR consists of a large cylindrical test section 3 m in diameter and 62 m long, which can be pressurized or evacuated to achieve the desired Reynolds number for the model size and velocity. The model is launched from a light-gas gun located at one end on the test section, and travels in free flight down its length. Data are collected along the flight path of the model by orthogonal, direct-shadowgraph systems located at 24 stations irregularly spaced over its length between 2.1 m to 4.2 m intervals. All of the optics are internal to the tank, which imposes a limit on the maximum velocity of the model because of fogging problems when the gas radiates. Many tests in this facility are conducted with powder-gas guns rather than with deformable-piston light-gas guns. A schematic of the facility is contained in Fig. 4. The advantages of this facility over HFFAF are threefold: long model trajectory, ambient pressures up to about 6 atm and highly detailed shadowgraphs. The operating characteristics of this facility are summarized in Table 3.

Slender Cone Drag Tests. Experiments have been conducted on sharp 5° and 10° half-angle cones at a Mach number of approximately 15 in the two ranges. The 5° data was recently acquired in the HFFAF, while the 10° data obtained in the PBR has been reported in Ref. 2. Drag coefficients have been obtained using both a linearized data reduction routine as well as a more sophisticated 6-degree-of-freedom data reduction routine, which can identify the effects of angle of attack and velocity on the total drag. Results of the two methods are consistent. Drag coefficients are compared with the results of a real gas computation and with ideal gas results. At the conditions of the experiments, skin friction drag makes up a significant portion of the total drag and can be affected by chemistry.

The effects of real gas chemistry on the drag of sharp, slender cones appear as an increase in the skin friction. In the case of the 10° cone at a Reynolds number of 400,000, about 40% of the total drag is due to skin friction.

Figs. 5 and 6 show shadowgraphs obtained for the 10° and 5° cones in free flight at the ballistic ranges. The computed shock angles compare well with the measured angles. Fig. 7 is a comparison of computed and measured drag coefficient for the 10° cone at a Reynolds number of 0.4×10^6 and Mach number of 15. The rms residual of the best fit for the trajectory of the 10° cone was 0.1 inches. The measurement accuracy for any ballistic range data is a function of the model size and shape, the clarity of photographs, and the skill of the film reader. Included in the figure are computed values of drag coefficient from ideal gas[3] and real gas[4] parabolized Navier-Stokes (PNS) codes and the ideal gas pressure drag value from Sims.[5] The pressure drag contributes about 40% of the total drag at zero angle of attack. The real gas drag coefficient is slightly higher than the ideal gas value although the computation agrees very well with the experiment for this case. Generally the computational results fall below the experimental values. Comparable agreement was found between computation and experiment for the more recently acquired 5° cone data.

During the course of comparing the computer solutions with experimental results, we made several observations relating to code calibration and validation. When comparing absolute values, such as drag coefficient, all sources of experimental, as well as computational, error must be evaluated. For example, since drag is sensitive to Reynolds number, the measurement accuracy of that number as well as that of other input parameters should be evaluated. In one case a 10% change in calculated Reynolds number resulted in a 6.5% change in the drag coefficient. This is outside of the experimental error range and could make comparison between theory and experiment meaningless. Since all initial and boundary conditions used in a computation cannot or have not been measured, code sensitivity to these conditions should be explored. All sources of error in the experimental data should be documented. The sensitivity of the computer code to grid size and shape, and to initial and boundary conditions, should be well documented. This is especially true when people other than the code developers are running the code.

Finally, while aerodynamic coefficients give a gross indication that a computer code can properly simulate a flow field, detailed flow-field quantities (such as density, temperature, and species concentration) must be measured if problems within the computational solution are to be identified and corrected. These kinds of measurements are difficult to obtain in the ballistic range. Modern diagnostic techniques are now available, however, that make such measurements feasible. At the present time a laser holographic system is being installed in the HFFAF which will permit the determination of the density field from interferogram fringe patterns. Techniques to determine model wall temperature are also being studied, such as temperature sensitive paints, infrared photography, and telemetered data. These additional data will permit code validations as well as calibration by the drag data discussed above.

Galileo Tests. The ballistic ranges have also supported all of the United States' probe missions to other planets. These include the 1976 Viking mission to Mars and the 1978 Pioneer Venus mission. Currently, tests are being conducted on the Galileo probe. The Galileo spacecraft will be launched in the near future and will arrive at Jupiter 2 years later. The probe will make in situ measurements as it descends through the Jovian atmosphere prior to its eventual destruction caused by extreme external pressures.

Although the probe aerodynamics were needed initially for design purposes, more accurate aerodynamics are needed in support of the Atmosphere Structure Experiment carried on board the probe. This experiment is designed to determine the state properties (i.e., density, pressure, temperature) of an unknown planetary atmosphere as functions of altitude from measurements made during the entry and descent of a probe. The experiment consists of a three-axis accelerometer, plus pressure and temperature sensors. During the high-speed portion of the trajectory, from an entry velocity above 47 km/sec to sonic speed, direct measurements are impractical and accelerometers are used to determine the state properties. This requires the precise knowledge of the probe aerodynamics, in particular the vehicle drag and lift coefficients as functions of Mach number and Reynolds number. The aerodynamic characteristics plus the measured decelerations allow the probe attitude to be determined and the atmospheric density to be deduced. Integration of the density gives the pressure, and the temperature is deduced from the equation of state (given the molecular weight, which is measured by another onboard experiment). The ballistic range facilities are well suited to providing the accurate aerodynamic data over a wide range of conditions.

A typical shadowgraph of a Galileo model in flight obtained in HFFAF is shown in Fig. 8. The screw on the model base is for attachment to its sabot prior to launch. The vertical wires are plumb lines for reference, and the irregular markings are imperfections in the facility windows caused by past debris impacts.

Low-Reynolds-Number Tests. Tests are also being conducted to precisely define the drag characteristics of the Galileo probe at Reynolds numbers, based on model diameter, of about 500 to 250. Obtaining drag data at these low Reynolds numbers is important because the drag coefficient is expected to increase markedly as the slip-flow and free-molecule-flow regimes are approached. This dramatic increase in drag coefficient occurs below a Reynolds number of about 1000.

The importance of obtaining drag data at various Reynolds numbers is shown in Fig. 9. Shown are Pioneer Venus data[6] down to a Reynolds number of about 250. The drag coefficient increases continuously below a Reynolds number of 1 million, but the increase becomes most dramatic below 1000.

AOTV Tests. Ballistic range tests have been conducted for two AOTV configurations: a symmetric and a raked-elliptic-cone configuration. These tests were conducted to: 1) provide experimental aerodynamic data and good flow-field definition against which computational aerodynamicists could validate their computer codes, 2) define bow shock wave shape and shock standoff distance, 3) investigate flow impingement on the afterbody, 4) compare the aerodynamics of several configurations, 5) investigate how minor changes in corner geometry affect the flow field, 6) determine the trim angle of attack of a trimmed vehicle.

A shadowgraph for the symmetric configuration[6] is shown in Fig. 10 and for the raked elliptic cone[6] in Fig. 11. These flow visualizations along with drag data from these tests are used for computer code calibration. With the newer holographic techniques, density data can also be used for code validation.

Other Tests. Simple shapes (such as sharp and blunt cones, bi-cones, and blunt bodies) are used in the ballistic ranges and sting mounted in shock tubes and tunnels to study the effect of real gas properties. Real gas thermodynamic and transport properties and finite rate chemical reactions have a pronounced effect on shock and Mach wave positions and shapes, emitted radiation, and aerodynamic drag. A detailed survey of simulation and diagnostic techniques used for these studies was presented by Sharma and Park.[7]

Transition Studies. In the past, transition studies were made in the HFFAF. Shadowgraph data on models launched in the range clearly show transition onset (e.g., Ref. 8), and measurements of total drag show the effect of low density in increasing drag coefficient. These transition studies will be continued on slender cone, bi-cone, and tri-cone shapes as well as on slender bodies.

Shock Tunnel

The 16-in. combustion driven shock tunnel, which provides the counterflow capability for the ballistic range, consists of a 23-m long, 43-cm diam driver section followed by an 26-m long, 30-cm diam driven section. It is capable of producing enthalpies corresponding to flight at Mach 15 and, because of the long, large diameter driver and driven sections, can produce a run time typically of 25 msec when operated at tailored-interface conditions. The flow from the shock tube is expanded through a Mach 7 axisymmetric nozzle through a test section which is 27 m long and 1 m across. The operating characteristics of this facility have been summarized in Table 2, and are described in detail in Ref. 1.

Hypersonic Boundary Layer Studies. Hypersonic boundary layer studies can be made in the HFFAF shock tunnel. The tunnel length of 27 m results in Reynolds numbers as high as 80×10^6. Tunnel wall boundary layer surveys can determine species, density, and velocity distributions and surface measurements can determine pressure, temperature, and heat flux.

Nozzle/Plume Experiments. Real gas nozzle/plume flow-field experiments are being designed for the Mach 7 shock tunnel. Detailed flow-field measurements including velocity, density, and species distributions will define plume structures as will shadowgraphs and holograms. Surface pressure, heat flux, and streamlines will define the nozzle flow. Momentum loss measurements will be made where possible to determine performance characteristics. By loading the driven section with hydrogen-air mixtures it will be possible to simulate hypersonic air-breathing propulsion systems. Both nozzle expansion studies (with hydrogen-air combustion products) and combustor process studies are being planned. New optical diagnostic instrumentation will permit the measurement of species and temperature distributions, which will be critical for code validation purposes.

Arcjets/Combustion Experiments

Hydrogen-air combustion processes are studied in the 20-MW Panel Test Facility where an oblique detonation wave will be established in a supersonic stream consisting of a mixture of hydrogen and air. This experiment and preliminary computations are described by Cambier et al.[9,10] and Adelman et al.[11]

The 20-MW arc-jet facility consists of an arc heater supplied continuously with high-pressure air. The arc chamber can be pressurized to 10 atm. Air leaving the arc heater passes through a semi-elliptical nozzle with an exit area ratio of 36. A schematic of the test configuration is shown in Fig. 12. Enthalpies can range from 5 to 35 MJ/kg and air flow is variable from 0.05 to 0.68 kg/s. Nominal test conditions for the oblique detonation wave engine (ODWE) experiment correspond to maximum pressure and minimum current. Upgrading of the facility from 10 atm stagnation pressure to 40 atm is now in progress. This higher pressure will allow a closer simulation of the conditions expected at the inlet of a supersonic combustor. A five-stage steam ejector pump maintains test cell pressures down to 13 Torr.

The analysis of the ODWE has many levels of sophisticaion ranging from one-dimensional, steady, perfect gas flow to two-dimensional, viscous, shock capturing codes with finite rate chemistry. These codes are used to guide an experimental program aimed at proving the existence of oblique detonation waves and their use in supersonic combustors. The codes can, in turn, be validated by the resulting experimental data.

Proof-of-concept studies of the ODWE are designed to experimentally create and stabilize oblique detonation waves. The NASA Ames arc-jet hypersonic wind tunnel facilities can simulate combustor inlet conditions of Mach number and enthalpy. However, they cannot currently reproduce the expected pressures. Therefore it was necessary to determine if the low pressures would prevent the establishment of a detonation wave. This verification was carried out in several ways. The simplest method utilized a one-dimensional, steady flow, finite rate chemistry program [9] which calculated ignition delays and combustion behavior behind a 30° oblique shock wave.

The results of these calculations, which are shown in Fig. 13, demonstrate the strong dependence of ignition delay and combustion rate on pressure and temperature. As temperature and pressure are increased, combustion occurs closer to the oblique wave. However, this program does not simulate any coupling between heat release and wave angle, so the question remains whether a detonation has been created. Some estimates of coupling can be made by generating characteristics in the combustion zone and determining their intersections with the shock. If these characteristics do not intersect the shock within the bounds of the combustion chamber, then there is not enough coupling to be classified as a detonation. Instead, there is shock-induced combustion.

For the nominal experimental conditions, the gas exits the nozzle at Mach 4.6 at a pressure of 0.016 atm and a temperature of 840 K. Combustion behind a 30° oblique wave takes about 0.5 msec corresponding to a distance normal to the shock of approximately 5 cm. The closest characteristics originating from the combustion front would intersect the oblique shock at a point about 20 cm normal to the base of the wedge. This distance would correspond approximately to the height of the test section. Raising the pressure by a factor of 5 shortens the distance to about 0.7 centimeters. Characteristics would then start to intersect the oblique wave at a point 3.5 cm vertically above the base of the wedge. This coupling should create a detonation. Indeed, more sophisticated analyses employing fully coupled computational fluid dynamics and finite rate chemistry codes have shown the existence of a detonation under these conditions.[9]

The oblique waves will be created by a water-cooled wedge located approximately 1 ft downstream of the struts in the test section. Optical access is provided by 30-cm windows on either side of the test section, and a schlieren system will provide photographic records of the wave angle with and without fuel. Pressure and temperature transducers on the wedge will be used to measure the state of combustion behind the oblique wave.

Shock Tube Experiments

Shock tubes are unique in producing homogeneous high-temperature gas samples heated to an enthalpy and pressure calculable and selectable from the state of the undisturbed gas and measured shock velocity.

The electrical discharge heats either hydrogen or helium to a temperature of about 8000 K for hydrogen, and about 20,000 K for helium, without causing melting or ablation of the materials because the discharge time is very short. The maximum temperatures are set by the onset of ionization and accompanying energy loss by radiation. Compared to other heating methods, such as combustion, electrical heater, or adiabatic compression by a piston, the electrical arc-driven shock tube operating on this principle produces the highest shock speed.

The Electric Arc Shock Tube (EAST) Facility at Ames consists of one driver system and two parallel-driven tubes. One is a 10-cm i.d. tube 12 m in length, and the other is a 60-cm i.d. tube 21 m in length, both made of stainless steel. The driver can be operated in two configurations: 1) a 17.7-cm conical drive configuration with a 10.16-cm i.d. exit, and 2) a variable length (34 - 137 cm) 10-cm i.d. cylindrical configuration. The length of the cylindrical drivers can be varied by using a Lexan filler plug. A schematic of the facility is shown in Fig. 14.

Energy to the driver is supplied by a 1.24 megajoule 40 kV capacitor energy storage system. The 6-tier capacitor bank has 220 capacitors. By using different combinations of series-parallel connections, the capacitance of the bank can be varied from 861.3 μF to its maximum value of 6,126 μF. A diaphragm made of Mylar 0.35 to 0.50 mm in thickness separates the driver gas from the driven gas. It is ruptured because of the rise in pressure within the driver during the time the capacitor discharges.

The 24-inch EAST facility operates at pressures between 7 and 30 μm of mercury to simulate flight altitudes between 68 to 81 km. Test firings show that: (1) shock velocities in excess of 13 km/sec are achieved at densities equivalent to altitudes of 80 km, (2) the hot driver gas emits radiation in the same pattern as observed in previous higher density, slower shock speed tests, and (3) the driver gas does not radiate at unanticipated spectral frequencies. The 4-in. EAST facility operates at initial pressures between 0.1 and 760 Torr. Nonequilibrium real gas effects in N_2 and O_2 can be simulated by operating it at initial pressures between 0.1 and 3 Torr with shock velocities ranging from 4 to 12 km/sec. With certain modifications these facilities will be able to produce spectrally clean test gases, which will be used to perform basic experimental investigations on thermo-chemical nonequilibrium with particular emphasis on vibrational energy excitation and nonequilibrium. A description of proposed tests and instrumentation is given by Sharma and Park.[7]

A total of 760 runs have been made to date. Of these, the conditions of 75 runs are shown in Fig. 15. These runs can be classified into three different categories: (1) air or a gas of similar molecular weight (argon, carbon dioxide) as the test gas in the 10-cm tube, (2) air or a gas of similar molecular weight as the test gas in the 60-cm tube, and (3) hydrogen as the test gas in the 10-cm tube. These three classes of operations occupy different regions in the velocity-pressure plot in Fig. 15. Test times for these runs range from 2 μsec to 20 μsec corresponding to flight speeds of 40 km/sec to 6 km/sec respectively.

In order to study chemical kinetics at low densities, emission, absorption, and scattering spectroscopic techniques are used. For accurate and reliable measurement, the test gas produced must be spectroscopically clean. For this reason the spectra of the test gas produced in the shock tubes were analysed using 99.99% pure nitrogen. The spectra of test gas, Fig. 16, were recorded in an aluminum tube and consist of vibrational bands from molecular species, CN, N_2, N_2^+, NO, and O_2^+. No iron or chromium lines are identifiable in the spectra. The peak at about 3883 Å is caused by the compounding of the (0,0) band of the CN violet system with band head at 3883 Å and the (0,0) band of the first negative band of N_2^+ with band head at 3914.4 Å. The carbon element in the CN molecules is believed to have originated from the carbon dioxide and hydrocarbons contained in the test gas, vacuum pump oil vapors, and the Mylar diaphragm. Near the red end of the spectra, the first negative bands of O_2^+ with a band head at 5631.9 Å are seen. The oxygen molecules are believed to have originated mostly from the test gas. The presence of O_2 also explains the NO-β bands with band heads at 3207, 3043 and 2754 Å in the ultraviolet region. Overall, the spectrum is dominated by the molecular bands of N_2^+. The present finding agrees with the results of the tests conducted at AVCO.[12] Two wavelength uv absorption spectroscopy (1100 Å - 1800 Å) will be used to measure the ground state number density and vibrational temperature in N_2 and O_2. Using gated diode arrays, emission spectra of the gases will be recorded in the spectral range of 2000 Å - 9000 Å. A detailed discussion of the measurements is given by Sharma and Park.[7] Solutions obtained by Park,[13] using a two-temperature gas model, are compared with this AVCO emission data in Fig. 17. These AVCO tests also will be repeated in the EAST facility.

3.5-Foot HWT Experiments

Hypersonic perfect gas code validation experiments consist of complete flow-field measurements about simple generic TAV configurations in the 3.5-Foot HWT. Data includes surface pressure, heat flux and streamline patterns (oil flow), shadowgraphs, and laser Doppler velocimetry (LDV) and pitot probe flow-field surveys. The free-stream Mach number is varied between 5 and 14, length Reynolds numbers between 1 and 25 million, and altitudes up to 210,000 ft. Fig. 18 shows an elliptic cross section, delta planform all-body hypersonic aircraft model, sting mounted in the test section, currently under investigation. Shown in Fig. 19 is a shadowgraph for a Mach 7.4 free stream. The angle of incidence is 15 degrees and the length Reynolds number is 15×10^6. Clearly discernible is the windward shock and the expansion fan emanating from the forebody/afterbody junction.

The Ames 3.5-Foot HWT is a closed-circuit, blowdown-type tunnel with a pebble-bed heater to heat the air to prevent liquefaction and with axisymmetric contoured nozzles to achieve the test Mach numbers. The tunnel is equipped with a model quick-insert mechanism for moving models (transit time as short as 0.5 sec) into and out of the air stream.

The test conditions for this ongoing study will include nominal free-stream Mach numbers of 5, 7, and 10 (the Mach 14 nozzle being redesigned); free-stream Reynolds numbers, based on model length of 3 ft, from 1.5×10^6 to 25×10^6 (laminar to turbulent flows); and model angles of attack of 0°, 5°, 10°, and 15° (attached and separated flows). For the complete investigation, flow-visualization data (shadowgraphs and surface oil-flow patterns), surface pressures, surface heat transfer, and flow-field surveys (probes and laser velocimetry) will be obtained for the all-body model both without and with control surfaces. The surveys by LDV are contingent upon the development of an LDV system for the 3.5-Foot HWT. A study in this facility has demonstrated that LDV capability can be used therein.

FLIGHT EXPERIMENTS

Aeroassist Flight Experiment

A forthcoming NASA flight experiment called the Aeroassist Flight Experiment (AFE) is planned for early in the next decade. Ames Research Center will participate in this experiment by constructing a large base of radiometric data for high-altitude, high velocity thermochemically nonequilibrated flow conditions. The AFE will be carried to orbit by the Space Shuttle and then deployed for the atmospheric data pass. Accelerated by an 18,000-lb thrust solid rocket motor, the vehicle will enter the atmosphere at nearly 10 km/sec and then experience approximately 500 sec of aerodynamic deceleration, during which a variety of flight data, including radiative and convective heating rates, will be gathered. The vehicle will exit the atmosphere at orbital speed and be recovered by the Shuttle Orbiter for return to Earth for postflight evaluation. As a preliminary to the design of a radiometer for this experiment, an approximate method for predicting both equilibrium and nonequilibrium radiative surface fluxes has been developed.[14] Spectral results for one trajectory state, a velocity of 10 km/sec at an altitude of 85 km, are shown in Fig. 20, where the spectral surface flux at a distance of 20.9 cm behind the shock front is plotted as a function of wavelength in the spectral region from 0.2 to 2.0 μm. An inspection of the figure reveals that the spectrum appears to be composed of a background continuum with a color temperature in the range of 7,000 K to 8,000 K (based on a flux maximum in the vicinity of 0.4 μm) on which is superimposed a complex structure of molecular bands and broadened atomic lines. The radiation calculation included 11 species (O_2, N_2, NO, O, N, N^+, O^+, N_2^+, NO^+, O_2^+, and e^-); some of the more apparent band-heads and lines from these species are identified in the figure. These results, and others like them, are used to develop the instrument parameters for the three different types of radiometers proposed for the experiment.

RAM-C Experiments

During the late 1960s three experimental probes were flown into the atmosphere at approximately satellite speed.[15–17] These probes, which were called the RAM-C tests, were sphere-cone configurations with a 0.1524-m nose radius, 9° cone half-angle, and a total length of 1.295 m. They were instrumented to measure electron number densities in the flow field. The second test, RAM-C II, is of particular interest because no ablation products were produced. This probe had a beryllium heat-sink nose cap and a Teflon-coated afterbody. Electron number densities were measured at four axial locations using microwave reflectometers and in the boundary layer using an electrostatic rake.

Computations were performed to replicate the RAM-C II tests at altitudes of 61, 71, and 81 km. This altitude range approximately spans a region of near-thermo-chemical equilibrium at 61 km to strong nonequilibrium at 81 km. The wall temperature was fixed at 1500 K, which is an approximation to the experimental wall temperature which is unknown. The wall was assumed to be fully non-catalytic which is also an approximation to the RAM-C II test. In each case the free-stream velocity was 7650 m/s.

The computations[18] were performed on body-fitted meshes with 35 points axially along the sphere-cone and 50 points in the flow field normal to the body. Figure 21 shows a typical mesh used for one of the test cases. The computations were performed using shock-capturing for all cases.

Each case was computed using two different chemical models. One set of results was obtained considering five chemical species (N_2, O_2, NO, N, and O), and three vibrational temperatures (*i.e.*, one vibrational temperature per diatomic species). There are a total

of eleven coupled equations to be solved. The number density of electrons may be approximated with the use of the quasi-steady-state (QSS) assumption. A second set of results was computed for this gas with NO ionized. In this case there are seven species (N_2, O_2, NO, NO^+, N, O, and e^-), four vibrational temperatures, and the electron temperature, for a total of fifteen equations to be solved. The purpose of performing both sets of calculations is to compare the effects of the electrons on the flow field.

The computed results are first compared to the peak electron number density measured axially along the body at each altitude. These results are presented in Figs. 22 to 24. They show that the electron number density is highest at the nose and falls off rapidly around the shoulder of the body. The QSS approximation and the nonequilibrium approach follow this trend, but the latter method predicts the data much better. The QSS technique works best at lower altitudes because the flow field is closer to equilibrium for these cases. Conversely, the agreement between the experiment and the nonequilibrium results is best for the higher, nonequilibrium cases. The differences between the two computed results indicate the nature of a nonequilibrium flow field. As the gas expands around the shoulder of the sphere-cone, the translational temperature falls rapidly. The fluid carries with it a large number of electrons that have been produced near the nose but have not yet recombined. Thus, although the local temperature is relatively low, the number of electrons remains high in the shoulder region. This effect is captured by the seven-species solution. However, if we assume that the reaction producing the electrons is governed by the local temperature as in the QSS approach, we predict too few electrons.

Figure 25 compares the computed results using the seven-species model to the measured electron number density near the body surface at $x/r_n = 8.10$ for altitudes of 71 km and 81 km. The results are approximately the right magnitude but do not show the correct behavior near the wall. This problem is likely caused by the uncertainty in wall boundary conditions. The surface of the probe was probably catalytic for the electron-ion recombination reaction and thus would cause a lessening of the electron number density near the wall. This wall effect is not currently included in the calculations. Alternatively, the fixed-wall temperature used in the calculations may be too high which would produce an excessive number of electrons near the wall.

The electron number densities computed using the seven-species gas model are in good agreement with the RAM-C II flight experiment. The use of a QSS assumption to derive the electron density from the five-species model predicts the correct trend. However, this approach yields results that are typically at least an order of magnitude in error, especially in highly nonequilibrium cases. The computations also indicate that the heat transfer to the body in the nose region is about 50% greater for a reacting gas than for a perfect gas. The heat transfer results also show that for the cases studied, the flow field is adequately described by the five-species model unless an accurate representation of the electron density distribution is required. The vibrational state of the flow field may be approximated with only one vibrational temperature.

These results and others not discussed here demonstrate that the models used for the translation-vibration and electron-vibration energy exchange mechanisms are inadequate in the regime of the test cases. Further research is required to improve these models for high temperatures so that the vibrational and electron temperatures may be computed correctly.

Other Flight Experiments

Other flight experiments include the Fire 2[19] project where radiative emission power was measured at the stagnation point during the flight, and the PAET[20] flight where the radiation intensity in several narrow wavelength channels was measured at the stagnation point of a spherical nose re-entry body. Comparisons between each of these flight experiments and computed results by Park[21] (in which a two-temperature thermochemical nonequilbrium model for dissociating and ionizing air was used) are shown in Figs. 26 and 27, respectively.

RAREFIED FLOWS

Direct simulation Monte Carlo calculations are being used to study and validate nonequilibrium thermodynamic and transport models, slip-flow codes, and modified Navier-Stokes codes designed to accommodate the breakdown of the Stokes hypothesis. New algorithms based on kinetic theory concepts are also being studied and evaluated.

CONCLUDING REMARKS

The experimental program for validating real-gas hypersonic flow codes at NASA Ames has been described. Ground- based test facilities include ballistic ranges, shock tubes and shock tunnels, arc jet facilities and heated-air hypersonic wind tunnels. Flight test facilities consist of the Aeroassist Flight Experiment, the Space Shuttle, project Fire 2, and planetary probes such as Galileo, Pioneer Venus, and PAET. While any single experiment is not sufficient to validate a given code, the experimental program described herein, taken in total, should provide data over a broad range of conditions. Real gas computer flow codes which account for finite rate chemical reactions and thermal nonequilibrium can then, in part, be validated and calibrated by comparisons with data from the experiments identified in this program.

REFERENCES

1. Ballistic Range Technology. AGARDograph No. 138 (ed. Canning, T.N., Seiff, A., and James, C.S.).

2. Intrieri, P. F., Kirk, D. K., Chapman, G. T., and Terry, J. E., "Ballistic Range Tests of Ablating and Nonablating Slender Cones," AIAA J., Vol. 8, No. 3, Mar. 1970, pp 558-564.

3. Lawrence, S. L., Chaussee, D. S., and Tannehill, J. C., "Application of an Upwind Algorithm to the PNS Equations," AIAA Paper 87-1112, Honolulu, HI, June 1987.

4. Prahbu, D.K, Tannehill, J.C., and Marvin J.G., "A New PNS Code for Three-Dimensional Chemically Reacting Flows," AIAA Paper 87-1472, Honolulu, HI, June 1987.

5. Sims, J.L., "Tables for Supersonic Flow around Right Circular Cones at Zero Angle of Attack," NASA SP-3004, 1964.

6. Intrieri, P.F. and Kirk, D.B., "High-Speed Aerodynamics of Several Blunt-Cone Configurations," AIAA Paper 86-0300, Reno, NV, Jan. 1986.

7. Sharma, S.P. and Park, C., "A Survey of Simulation and Diagnostic Techniques for Hypersonic Nonequilibrium Flows," AIAA Paper 87-0406, Reno, NV, Jan. 1987.

8. James, C. S., "Observations of Turbulent-Burst Geometry and Growth in Supersonic Flow," NACA TN 4235, Apr. 1958.

9. Cambier, J-L., Adelman, H. G., and Menees, G. P., "Numerical Simulations of Oblique Detonations in Supersonic Combustion Chambers," 8th International Symposium on Air-Breathing Engines, June 1987, Cincinnati, OH, also submitted to the AIAA Journal of Propulsion and Power.

10. Cambier, J-L., Adelman, H. G., and Menees, G. P., "Numerical Simulations of an Oblique Detonation Engine," AIAA Paper 88-0063, Reno, NV, Jan. 1988.

11. Adelman, H. G. and Menees, G. P., "Analytical and Experimental Validation of the Oblique Detonation Engine Concept," AIAA Paper 88-0063, Reno, NV., Jan. 1988.

12. Camm, J.C. and Rose, P.H., "Electric Shock Tube for High Velocity Simulation," AVCO Everett Research Laboratory, Research Report No. 136, July 1962.

13. Park, C., "Assessment of Two-Temperature Kinetic Model for Dissociating and Weakly Ionizing Nitrogen," AIAA Paper 86-1347, Boston , MA, June 1986.

14. Davy, W.C., Park, C., Arnold, J.O., and Balakrishnan, A., "Radiometer Experiment for the Aeroassist Flight Experiment," AIAA Paper 85-0967, Williamsburg, VA, June 1985.

15. Akey, N. D. and Cross, A. E., "Radio Blackout Alleviation and Plasma Diagnostic Results From a 25,000 Foot per Second Blunt-Body Reentry," *NASA TN D-5615*, Feb. 1970.

16. Grantham, W. L., "Flight Results of 25,000 Foot per Second Reentry Experiment Using Microwave Reflectometers to Measure Plasma Electron Density and Standoff Distance," *NASA TN D-6062*, Dec. 1970.

17. Jones, W. L., Jr. and Cross, A. E., "Electrostatic Probe Measurements of Plasma Parameters for Two Reentry Flight Experiments at 25,000 Feet per Second," *NASA TN D-6617*, Feb. 1972.

18. Candler, G. and MacCormack, R., "The Computation of Hypersonic Ionized Flows in Chemical and Thermal Nonequilibrium," AIAA Paper 88-0511, Reno, NV, Jan. 1988.

19. Cauchon, D. L.,"Radiative Heating Results from the Fire 2 Flight Experiment in a Reentry Velocity of 11.4 Kilometers per Second," NASA TM-X 1402, 1967.

20. Whiting, E. E., Arnold, J. O., Page, W. A., and Reynolds, R. M., "Composition of the Earth's Atmosphere by Shock-layer Radiometry During the PAET Entry Probe Experiment," J. Quantitative Spectroscopy and Radiative Transfer, Vol. 9, Sept. 1973, pp. 837-859.

21. Park, C., "Assessment of Two-Temperature Kinetic Model for Ionizing Air," AIAA Paper 87-1574, June 1987.

TABLE 1. HYPERSONIC FLOW CODE VALIDATION ACTIVITY

Code	Validation activity	Facility
Perfect gas	Generic TAV configurations	3.5 ft HWT
	AOTV configurations	Pressurized ballistic range
Real gas	Cones and blunt bodies	HFFAF (ballistic range)
	Blunt body shock layer	Shock tubes
	Benchmark codes	CCF and NAS
Nozzle/plume	Multi-nozzle perfect gas	3.5 ft HWT
	Semi-direct connect test	HFFAF (16 in. shock tunnel)
Combustion	Oblique detonation wave	20 MW arcjet
Thermochemical Nonequilibrium	Shock tube data	E.A.S.T.
	Shock layer data	HFFAF and 60 MW arcjet
	Flight experiment	AFE
Boundary layer	Tunnel wall boundary layer	HFFAF (16 in. shock tunnel)
	Transition on cones	HFFAF (ballistic range)

TABLE 2. AMES RESEARCH CENTER HYPERSONIC FACILITIES HYPERSONIC FREE FLIGHT FACILITY TEST CONDITIONS

• Stream	
– Mach number	7 (or still air)
– Static pressure	0.005 to 2 atm
– Enthalpy, max.	3000 Btu/lb
• Reynolds number	80,000,000 ft^{-1}
• Model	
– Velocity, max.	30,000 ft/sec
– Acceleration, max.	1,500,000 g
– size, max.	37 mm diam
– Weight, max.	45 g
• Instrumented range section	
– Diameter	3.5 ft
– Length	75 ft
– Number of stations	16

TABLE 3. AMES RESEARCH CENTER HYPERSONIC FACILITIES PRESSURIZED BALLISTIC RANGE TEST CONDITIONS

• Static range conditions	
– Gas composition	Air
– Pressure	0.1 to 1 atm
– Temperature	Ambient
• Reynolds number, max.	40,000,000 ft^{-1}
• Model	
– Velocity, max.	11,000 ft;sec
– Acceleration, max.	1,000,000 g
– Size, max	57 mm diam
– Weight, max.	100 g
• Instrumented range section	
– Length	203 ft
– Size, max.	20 in. wide X 20-60 in. high
– Number of stations	24

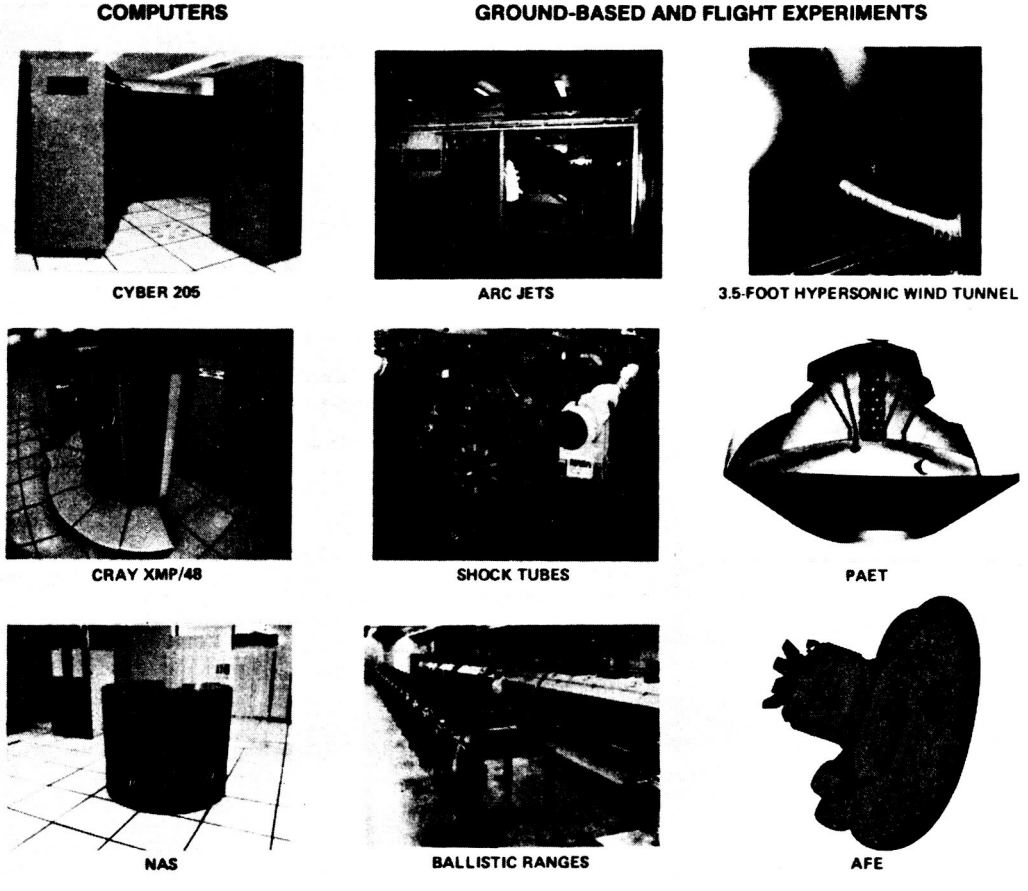

Figure 1 Facilities for studies in hypersonics and entry technology.

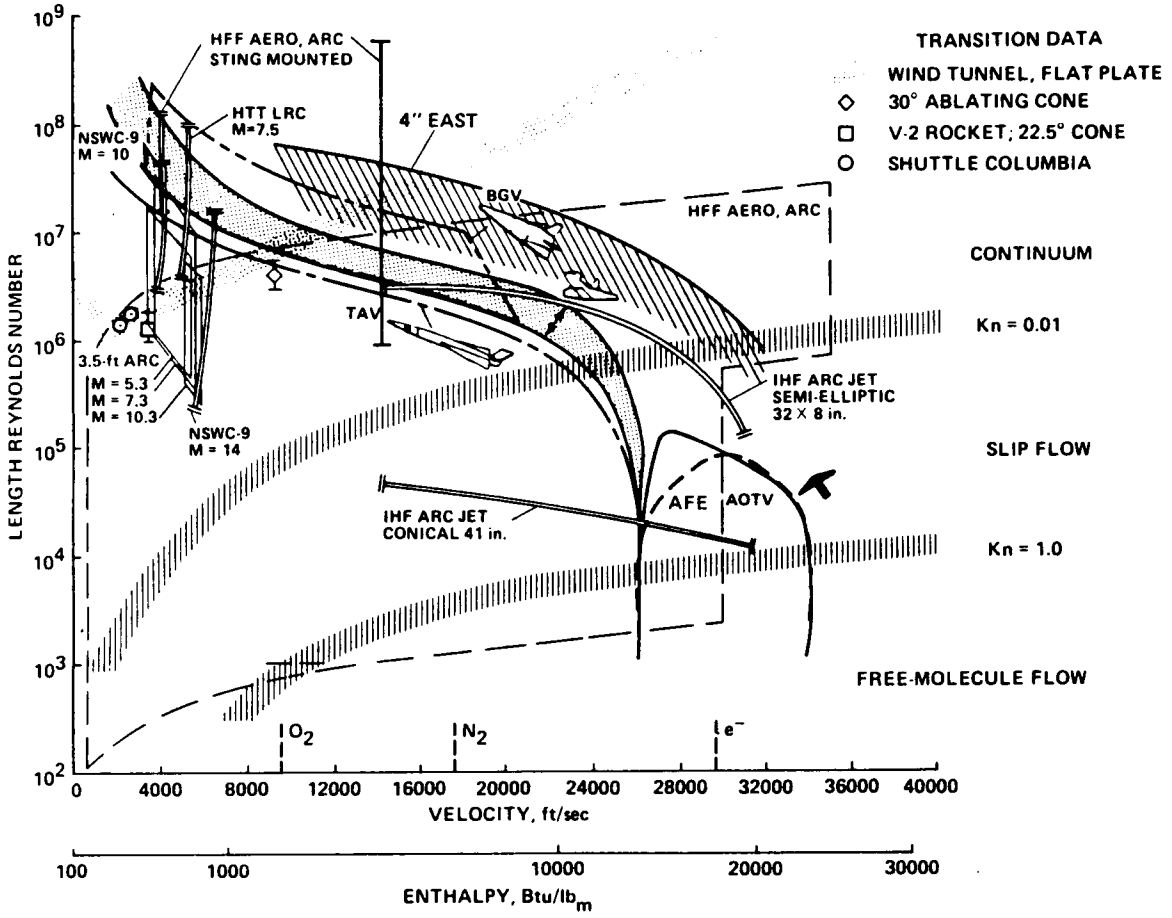

Figure 2 Flight domain simulation capability.

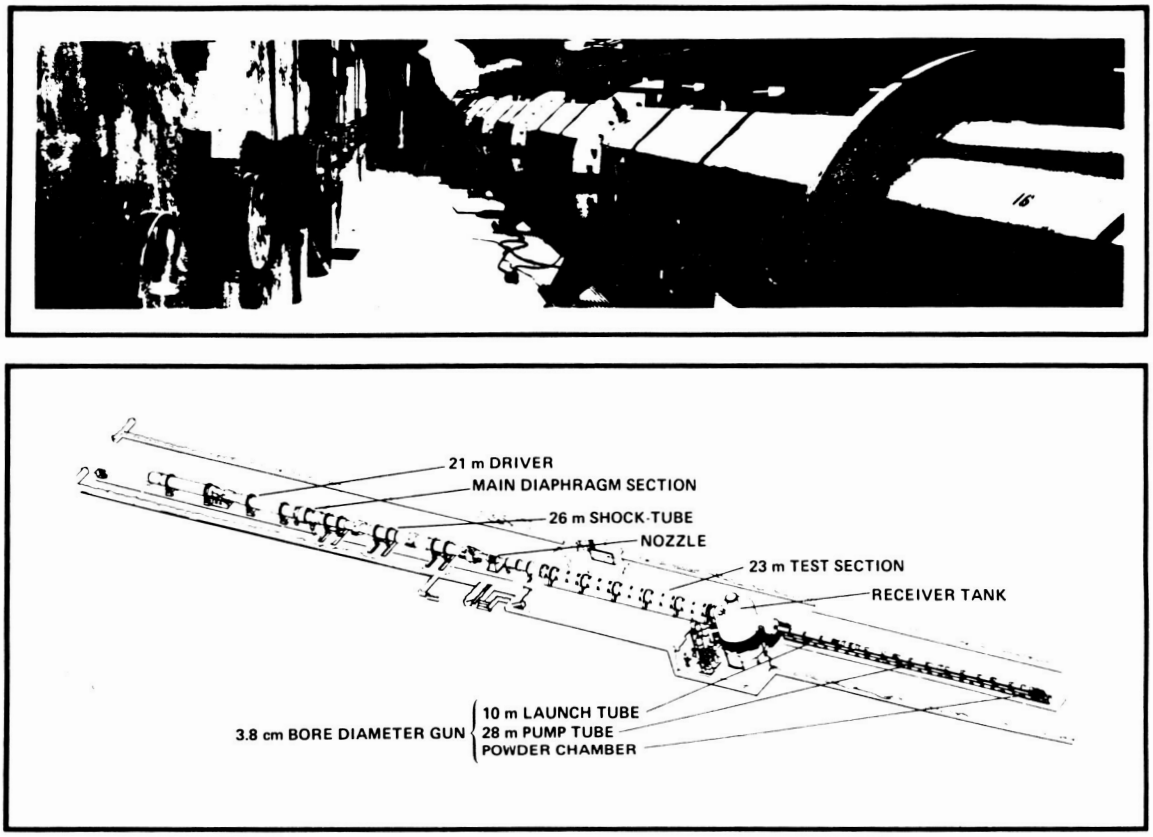

Figure 3 Hypersonic Free Flight Aerodynamic Facility.

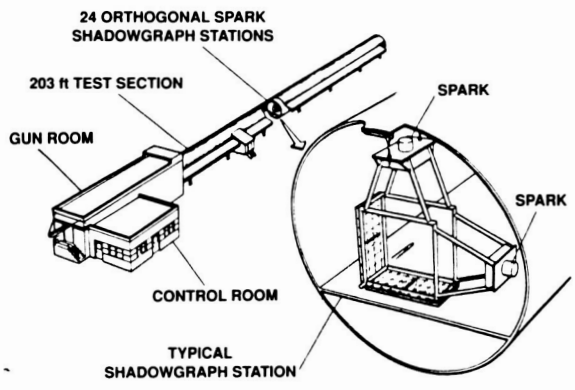

Figure 4 Pressurized ballistic range.

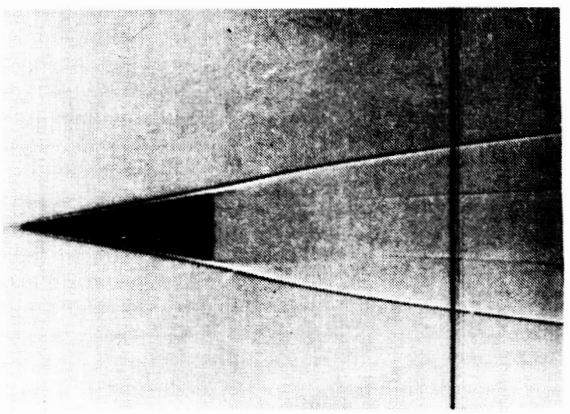

Figure 5 Shadowgraph of 10° cone at Mach 15.

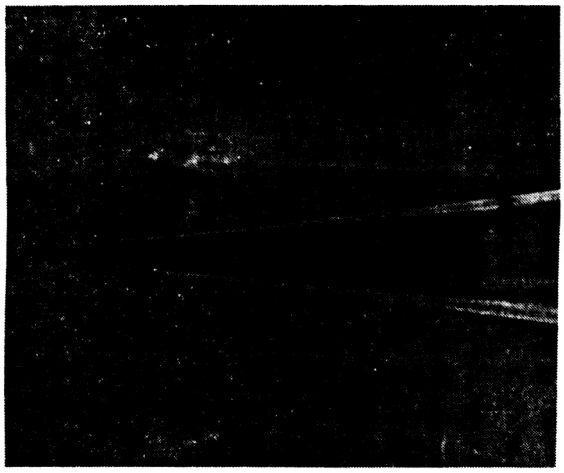

Figure 6 Shadowgraph of 5° cone at Mach 15.

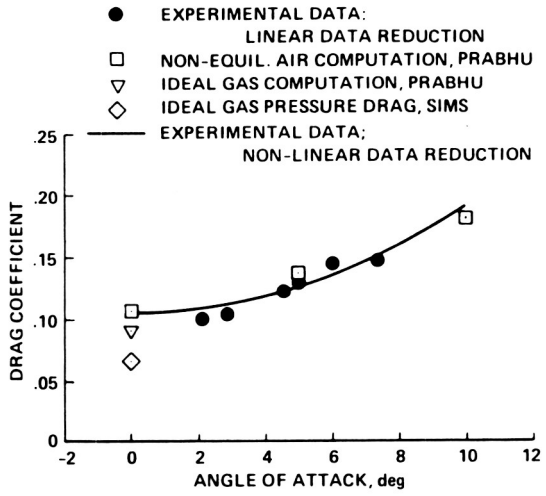

Figure 7 Drag data for 10° cone.

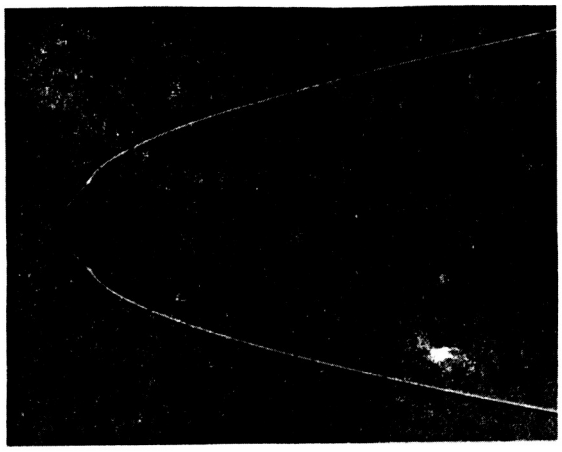

Figure 8 Shadowgraph of Galileo Probe. $M_\infty = 14$, $Re_d = 100{,}000$.

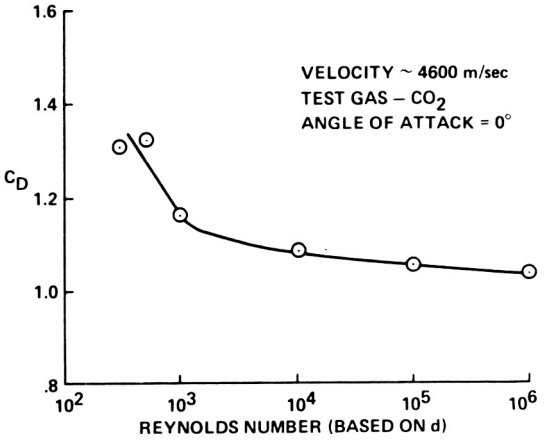

Figure 9 Effect of Reynolds number on drag characteristics of Pioneer Venus.

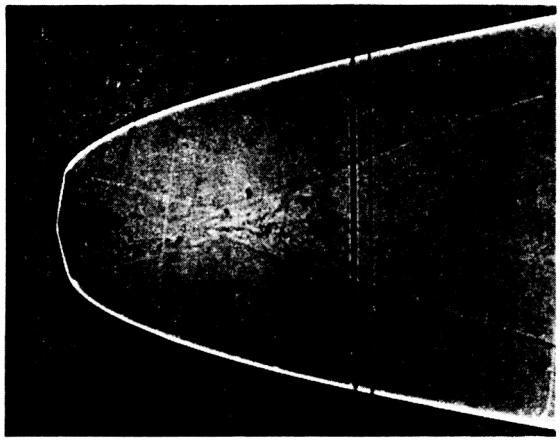

Figure 10 Shadowgraph of symmetric AOTV (Ref. 6).

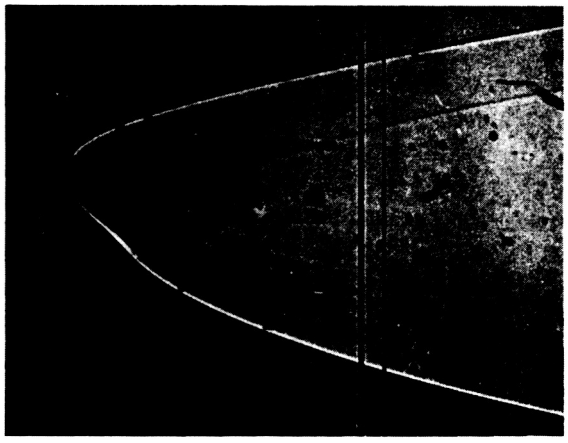

Figure 11 Shadowgraph of the raked elliptic cone (Ref. 6).

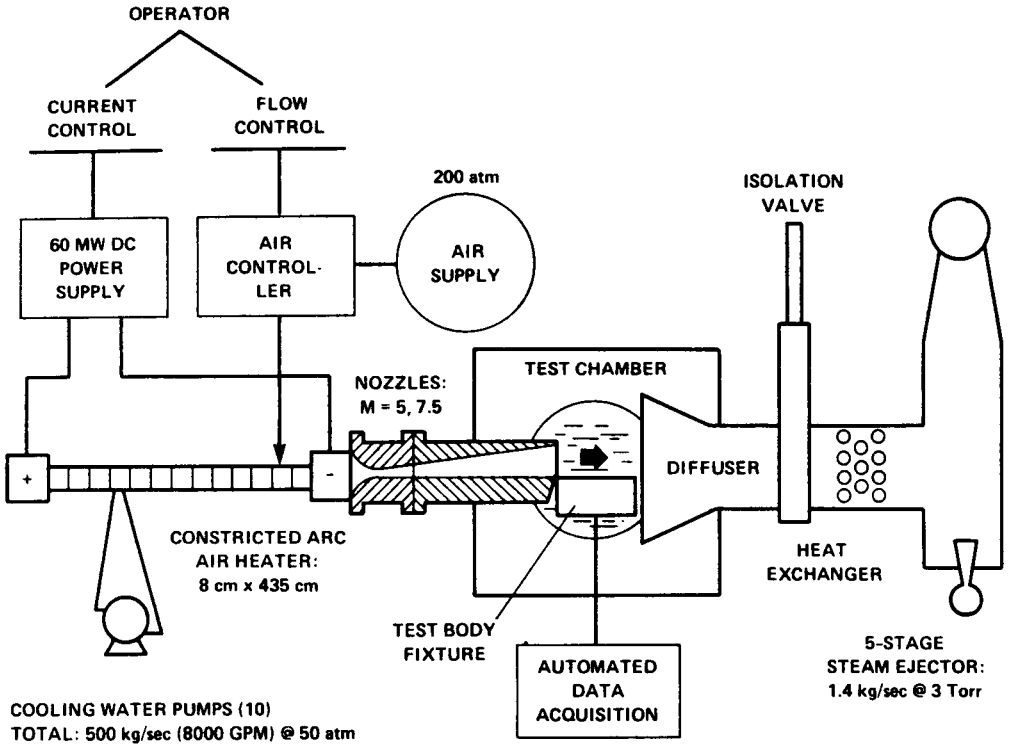

Figure 12 Schematic of interaction heating arcjet facility.

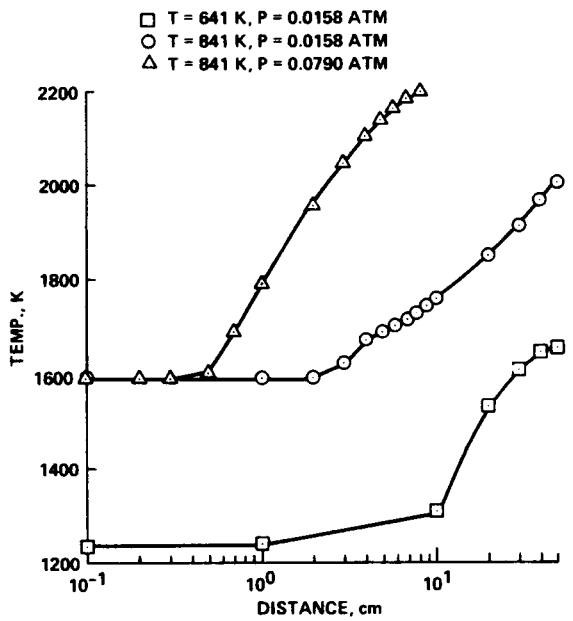

Figure 13 Computed combustion progress behind a 30° oblique shock wave.

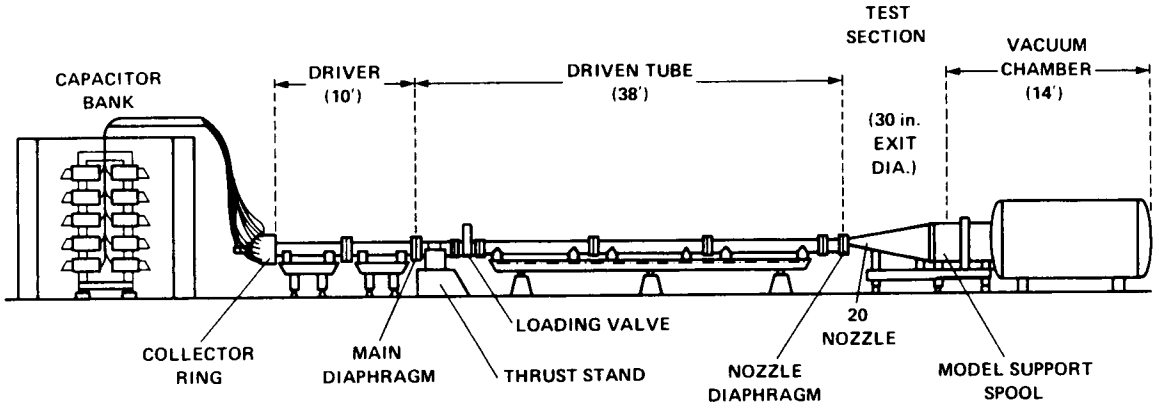

Figure 14 Schematic of Electric Arc-Shock Tube (EAST) Facility.

TUBE, cm	DRIVER GAS	DRIVEN GAS	DRIVER
▽ 10	He	AIR	30-in.
□ 60	He	AIR	30-in.
□ 10	H_2	H_2	54-in.
○ 10	H_2	H_2	CONICAL
◿ 10	He	Kr	54-in.
◺ 10	He	H_2/Ne	54-in.
□ 10	H_2	AIR	CONICAL

TUBE, cm	DRIVER GAS	DRIVEN GAS	DRIVER
○ 10	He	AIR	CONICAL
△ 60	He	AIR	CONICAL
◇ 10	N_2	AIR	CONICAL
△ 10	He	Ar	CONICAL
◇ 10	He	CO_2	CONICAL
⌂ 10	He	AIR	54-in.

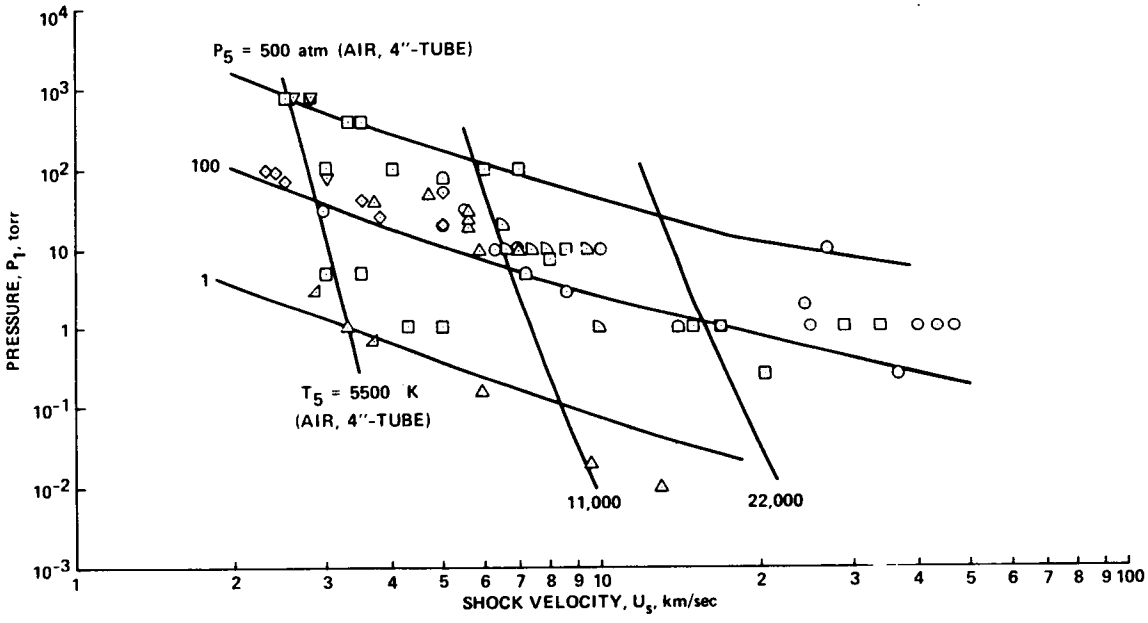

Figure 15 Measured shock velocity vs initial driven-tube charging pressure P_1.

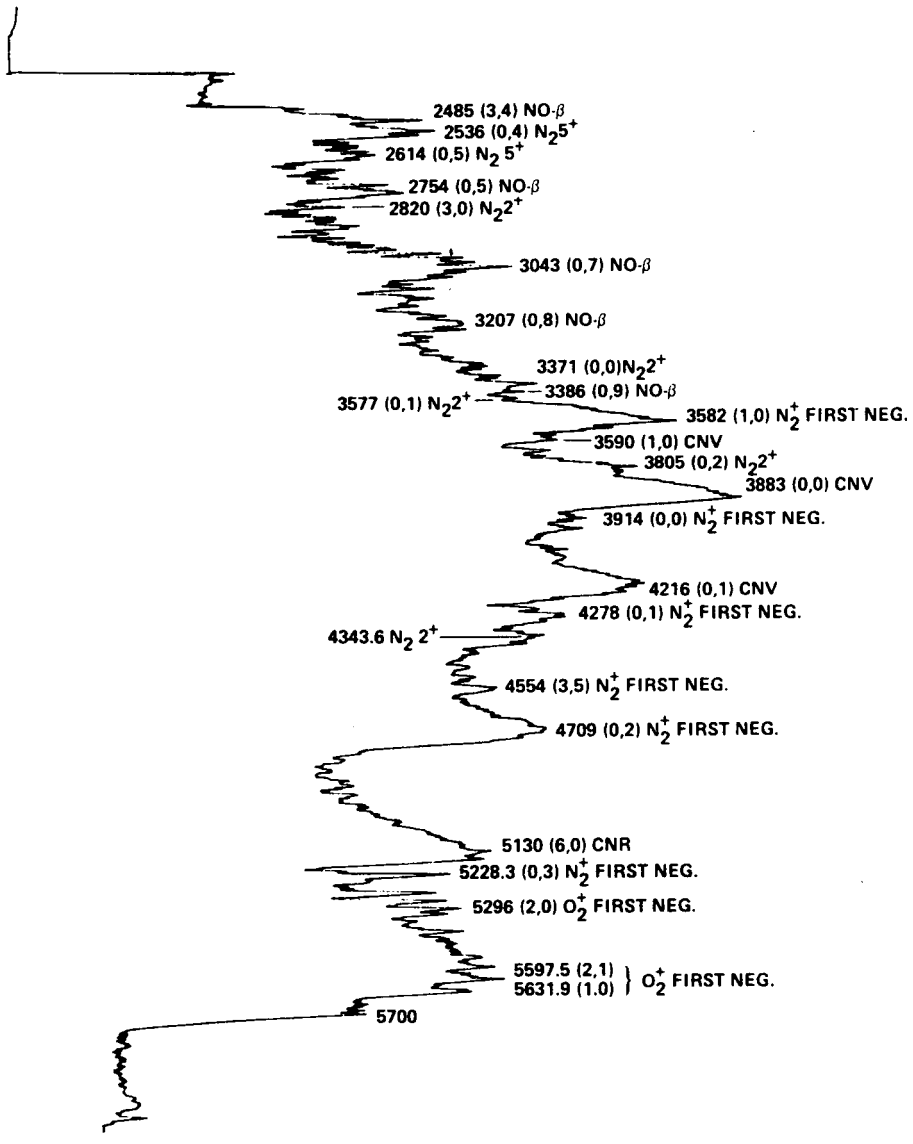

Figure 16 Emission spectra produced in the 10-cm driven aluminum tube. Initial drive pressure = 0.1 torr, shock velocity = 10.3 km/sec.

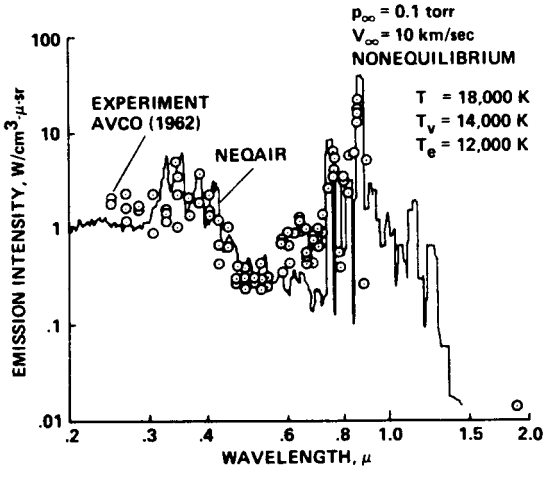

Figure 17 Comparison between calculated and measured spectra behind a plane normal shock wave.

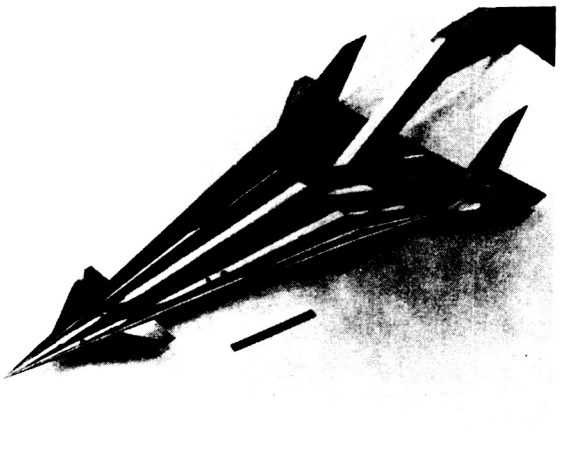

Figure 18 Generic all-body hypersonic aerospace plane model. 75° half-angle delta with elliptic cross section.

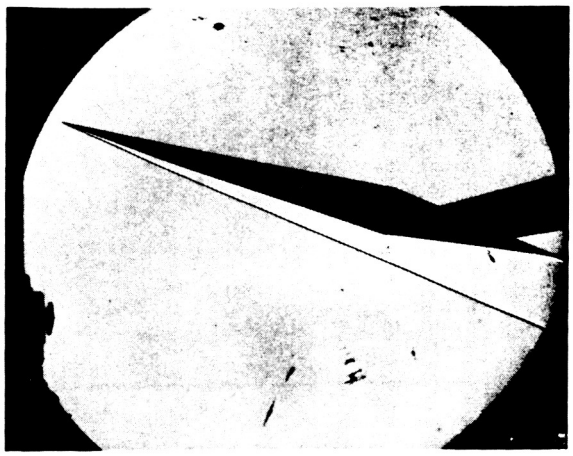

Figure 19 All-body model shadowgraph. α = 15°, M = 7.4 half-angle delta with elliptic cross section.

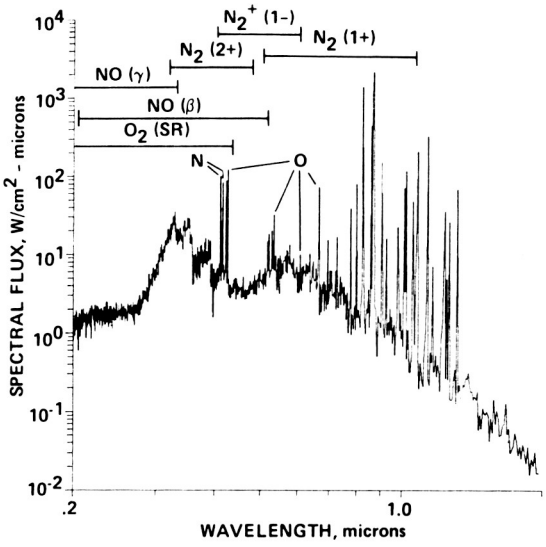

Figure 20 Nonequilibrium-flow spectral flux: shock-layer depth = 20.9 cm.

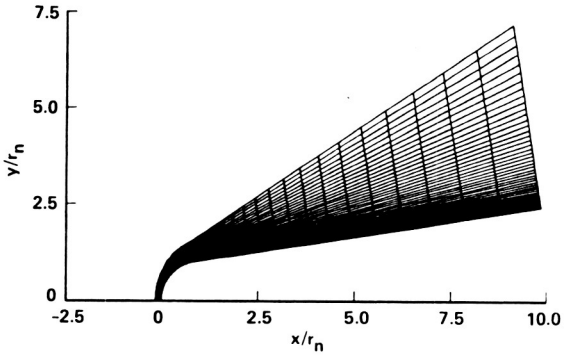

Figure 21 Computational grid for RAM-C.

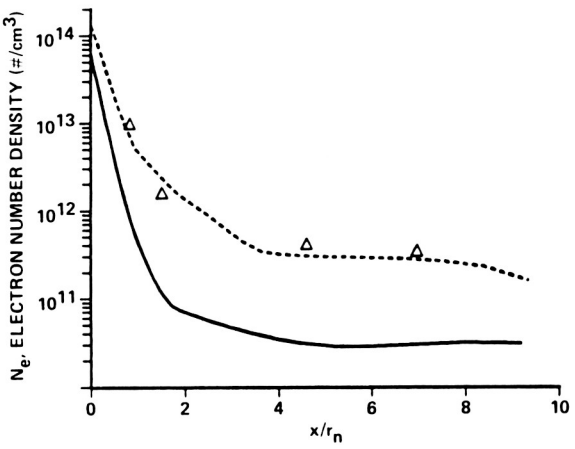

Figure 22 Comparison of peak electron number density. 61 km alt., M = 23.9.

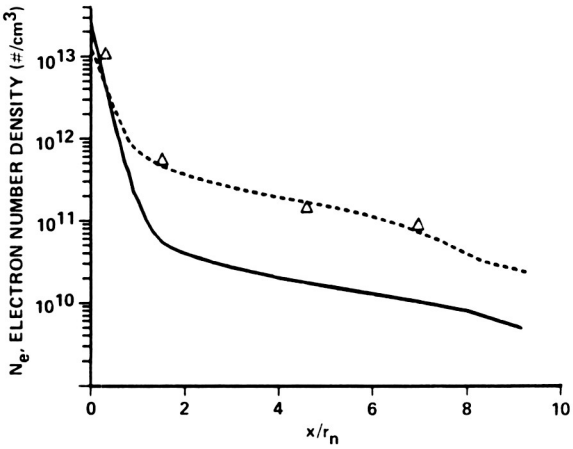

Figure 23 Comparison of peak electron number density. 71 km alt., M = 23.9.

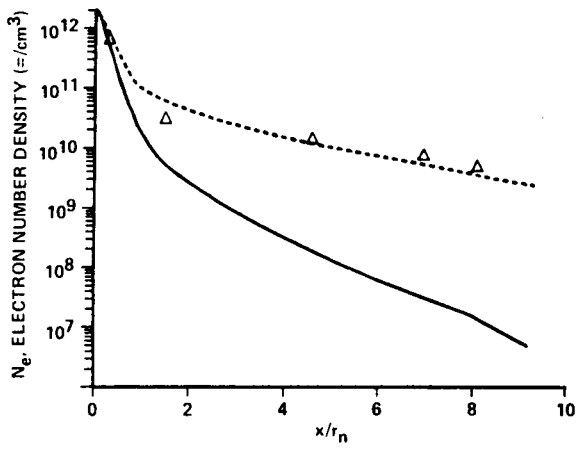

Figure 24 Comparison of peak electron number density. 81 km alt., M = 28.3.

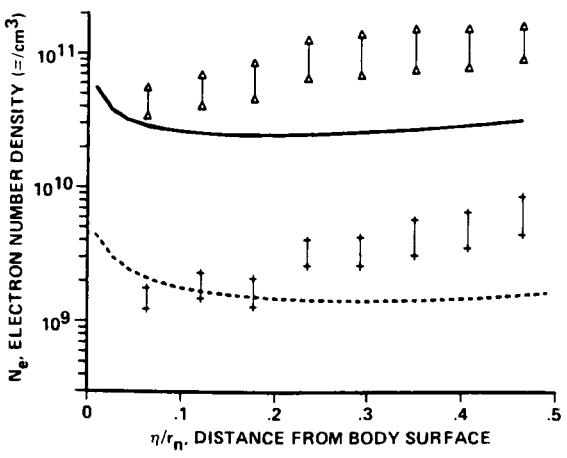

Figure 25 Comparison of electron number density distribution at $x/r_n = 8.1$.

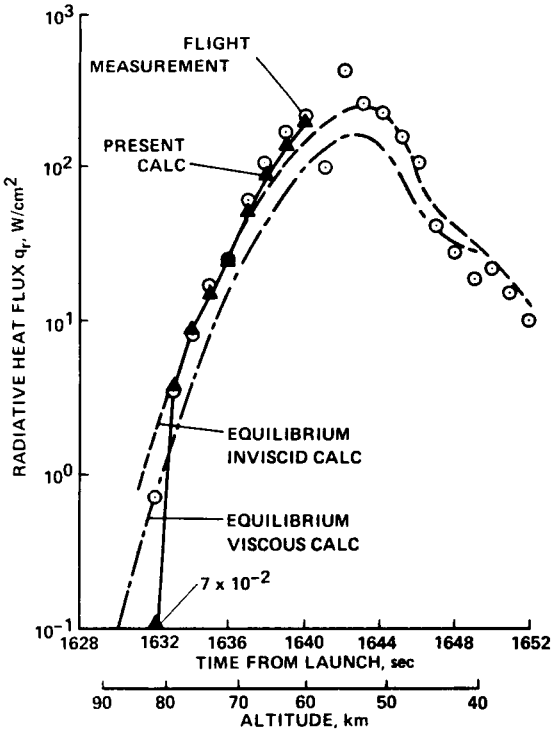

Figure 26 Comparison between calculated and measured stagnation-point radiative heat fluxes for Fire 2.

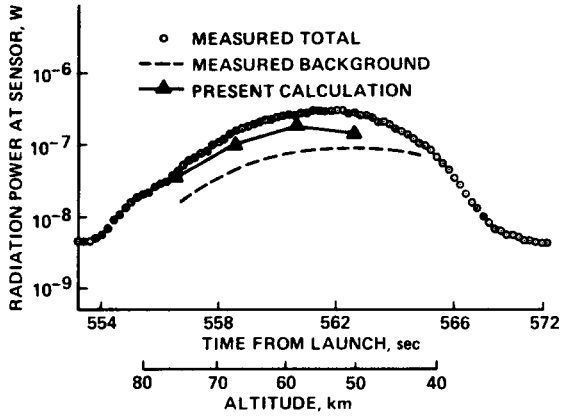

Figure 27 Comparison between calculated and measured radiation intensities at 391 nm in PAET experiment.

NASA
National Aeronautics and Space Administration

Report Documentation Page

1. Report No.	2. Government Accession No.	3. Recipient's Catalog No.
NASA TM-100093		

4. Title and Subtitle

Experimental Program for Real Gas Flow Code Validation at NASA Ames Research Center

5. Report Date

July 1989

6. Performing Organization Code

7. Author(s)

George S. Deiwert, Anthony W. Strawa, Surendra P. Sharma, and Chul Park

8. Performing Organization Report No.

A-88135

10. Work Unit No.

506-40-91

9. Performing Organization Name and Address

Ames Research Center
Moffett Field, CA 94035

11. Contract or Grant No.

13. Type of Report and Period Covered

Technical Memorandum

12. Sponsoring Agency Name and Address

National Aeronautics and Space Administration
Washington, DC 20546-0001

14. Sponsoring Agency Code

15. Supplementary Notes

Point of Contact: G. S. Deiwert, Ames Research Center, MS 230-2, Moffett Field, CA 94035
(415) 694-6198 or FTS 464-6198

Presented at AGARD Symposium on Validation of Computational Fluid Dynamics, Lisbon, Portugal, May 2-5, 1988

16. Abstract

The experimental program for validating real gas hypersonic flow codes at NASA Ames Research Center is described. Ground-based test facilities used include ballistic ranges, shock tubes and shock tunnels, arc jet facilities and heated-air hypersonic wind tunnels. Also included are large-scale computer systems for kinetic theory simulations and benchmark code solutions. Flight tests consist of the Aeroassist Flight Experiment, the Space Shuttle, Project Fire 2, and planetary probes such as Galileo, Pioneer Venus, and PAET.

17. Key Words (Suggested by Author(s))	18. Distribution Statement
Hypersonics Code validation	Unclassified-Unlimited Subject Category - 02

19. Security Classif. (of this report)	20. Security Classif. (of this page)	21. No. of Pages	22. Price
Unclassified	Unclassified	19	A02